

Doorway States in the Gamma Decay-Out of the Yrast Superdeformed Band in ^{59}Cu

C. Andreoiu,^{1,*} T. Døssing,² C. Fahlander,¹ I. Ragnarsson,³ D. Rudolph,¹ S. Åberg,³ R. A. E. Austin,⁴ M. P. Carpenter,⁵ R. M. Clark,⁶ R. V. F. Janssens,⁵ T. L. Khoo,⁵ F. G. Kondev,^{5,†} T. Lauritsen,⁵ T. Roderger,⁴ D. G. Sarantites,⁷ D. Seweryniak,⁵ T. Steinhardt,⁸ C. E. Svensson,^{6,*} O. Thelen,⁸ and J. C. Waddington⁴

¹*Department of Physics, Lund University, S-22100 Lund, Sweden*

²*Niels Bohr Institute, DK-2100 Copenhagen, Denmark*

³*Department of Mathematical Physics, Lund Institute of Technology, S-22100 Lund, Sweden*

⁴*Department of Physics and Astronomy, McMaster University, Hamilton, Ontario, Canada L8S 4M1*

⁵*Physics Division, Argonne National Laboratory, Argonne, Illinois 60439, USA*

⁶*Nuclear Science Division, Lawrence Berkeley National Laboratory, Berkeley, California 94720, USA*

⁷*Chemistry Department, Washington University, St. Louis, Missouri 63130, USA*

⁸*Institut für Kernphysik, Universität zu Köln, D-50937 Köln, Germany*

(Received 14 January 2003; published 5 December 2003)

The decay-out process of the yrast superdeformed band in ^{59}Cu has been investigated. The firm determination of spin, parity, excitation energy, and configuration of the states involved in this process constitutes a unique situation for a detailed understanding of the decay-out mechanism. A theoretical model is introduced that includes a residual interaction and tunneling matrix element between bands, calculated in the configuration-dependent cranked Nilsson-Strutinsky model. This interaction causes the decay to occur via a small number of observed doorway states.

DOI: 10.1103/PhysRevLett.91.232502

PACS numbers: 21.10.Re, 23.20.Lv, 24.10.-i, 27.50.+e

Superdeformed nuclear states are a manifestation of the shell structure in atomic nuclei [1,2]. At specific neutron and proton numbers, elongated superdeformed (SD) shapes are favored over normally deformed (ND) shapes. For the SD states to be pure, they need to be shielded from the ND states by an energy barrier in the deformation coordinates. During the emission of characteristic discrete γ rays from the SD rotational bands leading to lower angular momenta, the states of the elongated SD shape move up in energy relative to the more compact ND shape, and the barrier becomes lower and thinner. This eventually leads to decay-out of the band by a cascade of γ rays.

The shape change occurring in the decay-out implies a substantial rearrangement of nucleonic states. Especially the nucleonic states from higher shells, which are occupied in the SD bands, need to be vacated. This process is facilitated by vibrational coupling through the barrier between the SD state and doorway states [3], which in turn typically are coupled to a very large number of ND states [4]. Consequently, for the cases studied thus far in the mass $A \sim 190$ region, the decay-out is fragmented over numerous weak transitions as statistical cascades without any discernible selection rules [5–8]. The doorway states are masked by the chaotic character of the ND states.

The subject of the present Letter is to discuss the coupling between the SD band and the ND states displayed by the decay-out cascade in ^{59}Cu . Especially, we shall show that in this case a specific group of states couples directly to the SD band via the residual two-body interaction. These doorway states have been observed and are classified for the first time.

The high-spin states in ^{59}Cu were populated via the $^{40}\text{Ca}(^{28}\text{Si}, 2\alpha 1p)^{59}\text{Cu}$ fusion-evaporation reaction. The 122 MeV ^{28}Si beam was delivered by the ATLAS facility at Argonne National Laboratory. The 0.5 mg/cm² thin ^{40}Ca target was enriched to 99.975% and enclosed between two thin layers of Au to prevent oxidation. The experimental setup consisted of the Gammasphere array [9] comprising 103 Ge detectors, in combination with the 4π charged-particle detector array Microball [10]. The event trigger required the detection of at least four Compton suppressed γ rays. For details, see Ref. [11].

The yrast SD band in ^{59}Cu is connected to the low-spin ND states by numerous linking transitions, which have mainly stretched $E2$ character but also dipole character. This can be inferred from Fig. 1, which provides the significant part of the decay scheme of ^{59}Cu [11]. In fact, ^{59}Cu appears to be a somewhat fortuitous case, as the fragmentation of the full decay intensity can be studied throughout the decay steps. Another case, although not as complex, is ^{133}Nd [12].

The configurations of the observed regular bands in ^{59}Cu are well explained by the configuration-dependent cranked Nilsson-Strutinsky (CNS) approach [13,14] as discussed in detail in Ref. [11]. The orbitals important for the description of nuclei in the mass $A \sim 60$ region are introduced in Fig. 2: The $1f_{7/2}$ orbit below the spherical shell gap at $N = Z = 28$ and the upper (fp) shell (the $1f_{5/2}$, $2p_{3/2}$, $2p_{1/2}$ orbits) as well as the $1g_{9/2}$ orbit above the gap. All configurations are labeled according to $[p_1 p_2, n_1 n_2]$, where p_1 (n_1) is the number of proton (neutron) holes in the $1f_{7/2}$ orbit, while p_2 (n_2) denotes the number of $1g_{9/2}$ protons (neutrons). A more compact notation is $[q_1 \setminus q_2]$, with $q_1 = p_1 + n_1$ and $q_2 = p_2 + n_2$.

lowest $[3\setminus 1]$ configuration shown in Fig. 2 contains three odd particles placed in the $1g_{9/2}$, $\alpha = +1/2$, the (fp) , $\alpha = +1/2$ and the $1f_{7/2}$, $\alpha = -1/2$ orbitals. One proton and two neutrons can be put in these three orbitals in three different ways, yielding the three $[3\setminus 1]$ bands shown in Fig. 3(a). Shifting the signature of two of these orbitals preserves the total signature but requires an additional excitation energy determined by the signature splitting of the relevant orbitals in the rotating mean field. This energy amounts to ~ 2 MeV for the $1g_{9/2}$ orbital, ~ 0.5 MeV for the relevant (fp) orbital, and vanishing for the $1f_{7/2}$ orbitals. Hence, the next three bands of the $[3\setminus 1]$ configuration will be found at energies about 0.5 MeV higher than the ones included in the figure. Similar arguments can be applied to the $[2\setminus 1]$ bands.

At $I = 33/2$, the SD $[4\setminus 3]$ band and the three ND $[2\setminus 1]$ bands come close in energy [see Fig. 3(a)]. Since they differ only by a two-particle two-hole ($2p-2h$) excitation, one might expect a strong coupling between the SD band and these $[2\setminus 1]$ bands at this spin value leading to a decay-out already at $I = 33/2$. It seems, however, that this is prevented by a potential barrier. This is illustrated in Fig. 3(b), where the energy is shown along a straight line in the (ϵ_2, γ) plane, which approximately goes through the minima of the $[2\setminus 1]$, $[3\setminus 1]$, and $[4\setminus 3]$ configurations. At $I = 29/2$, no normal deformed state comes close to the SD state, while at $I = 25/2$ both the three $[3\setminus 1]$ bands and several excited $[1\setminus 1]$ bands [17] lie in the same energy range as the SD band. The $[1\setminus 1]$ states differ by (at least) a $3p-3h$ excitation from the states of the SD band, while all three $[3\setminus 1]$ states differ by a $2p-2h$ excitation. There is only a small barrier [cf. Fig. 3(b)] at this spin value between the SD state and the $[3\setminus 1]$ states. This suggests a strong coupling to the $[3\setminus 1]$ states, which then act as doorway states for the decay-out of the SD band.

To quantify these observations and to investigate the general structure of the decay-out flow of the SD band, the interaction between the states needs to be included explicitly and combined with transition matrix elements. We thus allow the bands to mix by introducing a residual two-body interaction in a similar way as in the models studied for damping of rotational bands (see Refs. [18,19]). Subsequently, the electromagnetic decay cascade is simulated. The observed decay mainly occurs via stretched $E2$ transitions, and only the states defined by the SD band and the positive parity, $\alpha = +1/2$ states involved in the decay-out between $I = 17/2$ to $I = 37/2$ are considered.

All 32 rotational bands shown in Fig. 3(a) are theoretically described by the occupation numbers of the (deformed and rotating) single particle orbits, the equilibrium deformations, and the correspondingly minimized energy for each spin. The residual interaction, \hat{V}_{res} , which takes into account the parts of the nuclear interaction not included in the mean field, implies a mixing between the rotational bands. This interaction must be of two-body nature, and it conserves the angular

momentum and parity quantum numbers. Denoting the unperturbed state as $|\mu, I^\pi\rangle$, where μ specifies the configuration and its deformation, the matrix elements of the residual interaction can be written as

$$\langle \mu', I^\pi | \hat{V}_{\text{res}} | \mu, I^\pi \rangle = V_{2p2h} \cdot T_{\text{coll}}(I). \quad (1)$$

The first term, V_{2p2h} , is due to the explicit change of configuration by a $2p-2h$ excitation, and the second term, T_{coll} , accounts for the change in the (collective) deformation between the two states μ' and μ . For V_{2p2h} , a two-body random matrix approach is applied and the matrix elements are chosen from an ensemble of Gaussian distributed random numbers with standard deviation $\sigma = 100$ keV. This choice for V_{2p2h} agrees with estimates made in other mass regions. For example, $V = 20$ keV in the mass $A \sim 160$ region [20] yields $V = 20 \times (160/60)^{3/2} = 87$ keV for the mass $A \sim 60$ region [18]. It is assumed that the matrix element V_{2p2h} is spin independent.

The second factor in Eq. (1), T_{coll} , takes into account the deformation change that may be more or less hindered by an energy barrier between the two energy minima. The potential energy barrier between the two states is calculated microscopically in the CNS model using the same theoretical description underlying the calculation of the unperturbed bands (see Fig. 3). If there is no barrier between the two states, we set $T_{\text{coll}} = 1.0$. The reduction of T_{coll} due to the barrier is calculated in WKB. In these calculations, we assume a dynamical mass, $B_\epsilon = 12 \cdot B_{\text{irr}}$ [1], and a zero point energy of 0.5 MeV. Obviously, T_{coll} is spin dependent, as is clearly demonstrated in Fig. 3(b). The large barrier at $I = 33/2$ between the SD state and the $[2\setminus 1]$ state, which results in $T_{\text{coll}} = 0.016$, has almost disappeared at $I = 25/2$. The barrier at $I = 25/2$ between the SD state and the $[3\setminus 1]$ state yields $T_{\text{coll}} = 0.15$.

The precise experimental information of transition energies and strengths in the four transitions out of the $29/2^+$ SD band allows for a direct determination of three of these matrix elements. One finds a rms value of 70 keV for the three matrix elements connecting the SD state at $25/2^+$ to the ND doorway states. Relative to our simulations, the stronger experimental matrix elements indicate a more open barrier at $25/2^+$.

The 32×32 matrix, describing the effective Hamiltonian, is set up and diagonalized for each spin value, and new eigenstates and energies are found. The new eigenstates, $|\alpha, I^\pi\rangle$, are linear combinations of the unperturbed states, $|\alpha, I^\pi\rangle = \sum_\mu a_{\alpha,\mu} |\mu, I^\pi\rangle$. To calculate the $E2$ decay we make the following assumptions: $B(E2)$ values for transitions along unperturbed bands are determined by the deformation of the band according to $B(E2) \sim [\epsilon \cos(\gamma + 30^\circ)]^2$, where the deformation is determined from the microscopic calculation averaged over the band. This gives $B(E2) = 200$ W.u. for the SD band ($\epsilon = 0.38$), and $B(E2)$ values between 14 and 78 W.u. for the different ND bands, which is consistent with derived experimental average quadrupole moments for bands 4

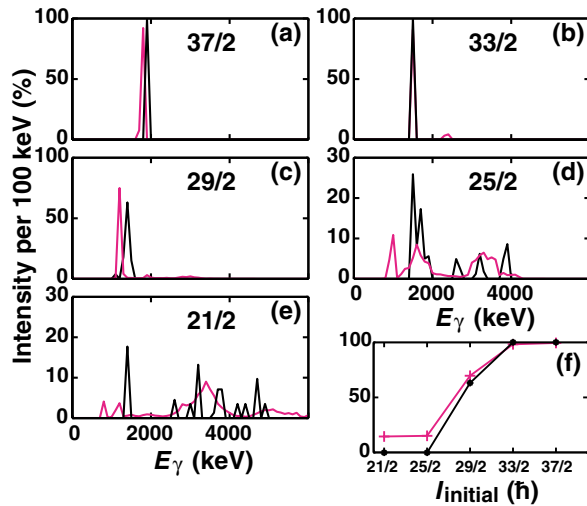


FIG. 4 (color online). Experimental (black line) and simulated (grey line) γ -ray spectra at initial spins $I_i = 37/2$ (a), $33/2$ (b), $29/2$ (c), $25/2$ (d), and $21/2$ (e) as a function of γ -ray energy. At $I_i = 33/2$, the two curves largely overlap. Panel (f) shows the simulated and measured intensity in the SD band as a function of spin, I_{initial} .

and 5 [11]. For transitions between unperturbed bands, which differ in configurations by $1p-1h$, we generically assume $B(E2) = 5$ W.u. Transitions involving a change of more than $1p-1h$ have $B(E2) = 0$, since the $E2$ -transition operator is of one-body character.

The $E2$ cascade is followed from the SD state at $I = 37/2$ which is initially given a 100% population. In the course of the decay, the intensity is spread over many mixed-band states as in the experiment (cf. Fig. 1). Results from such calculations are shown in Fig. 4. To exploit the random nature of V_{2p2h} , we show the sampling from 100 independent simulations of the interaction. The calculated γ -ray strengths are compared to the corresponding experimental strengths in Fig. 4 at initial spins $37/2$ (a), $33/2$ (b), $29/2$ (c), $25/2$ (d), and $21/2$ (e). In Fig. 4(f), the calculated and measured intensity in the SD band are compared.

The results of Fig. 4 can be interpreted with reference to the band energies displayed in Fig. 3. At spin $33/2$, the barrier effectively prevents a coupling to the three $[2\backslash 1]$ states, and only a small fraction of the decay, $\sim 1\%$, leaks out of the band at spin $33/2$. At spin $25/2$ there is a low barrier to the three doorway states of configuration type $[3\backslash 1]$, which as a result gives rise to four γ -ray transitions from the $29/2^+$ state to four $25/2^+$ states in both experiment and calculation. Two groups of transitions are seen with energies of about 1.8 MeV and 3–4 MeV for the $25/2 \rightarrow 21/2$ decay (cf. Fig. 1). The low-energy group, comprising transitions with relatively large $B(E2)$ values, corresponds to fragmented rotational strengths to the mixed $[3\backslash 1]$ and excited $[1\backslash 1]$ bands. The high-energy group reflects the cooling to the low-lying $[2\backslash 1]$ and $[1\backslash 1]$ states. The $21/2 \rightarrow 17/2$ transitions complete the

cooling down to the yrast line. The observed attenuation of the strength in the SD band is seen to be nicely reproduced by theory [cf. Fig. 4(f)]. The remaining strength at $25/2$ and $21/2$ in the calculation, which also is responsible for the lowest energy peaks around 1 MeV of the corresponding γ spectra, is an artifact of the truncation to the 32 states.

In summary, the observation of a multitude of linking transitions connecting the yrast SD band to low-spin states in ^{59}Cu have made possible a detailed understanding of the γ decay-out mechanism. It is found that the decay-out is caused by a direct coupling of SD states to a small number of doorway states. This provides another perspective of the decay-out process as compared to the heavier $A \sim 150$ and $A \sim 190$ regions, where the coupling to doorway states is masked by a chaotic environment of ND states, which leads to a very large number of linking transitions.

This research was supported by the Swedish Research Council, the Canadian NSERC, the U.S. DOE under Contracts No. W-31-109-ENG-38 (ANL), No. DE-AC03-76SF00098 (LBNL), and No. DE-FG05-88ER40406 (WU), and the German BMBF.

*Present address: Department of Physics, University of Guelph, Guelph, Ontario, Canada N1G 2W1.

†Present address: Technology Development Division, Argonne National Laboratory, Argonne, Illinois 60439, USA.

- [1] A. Bohr and B. R. Mottelson, *Nuclear Structure, Volume II* (Benjamin, New York, 1975).
- [2] A. G. Magner *et al.*, Phys. Rev. E **63**, 065201 (2001).
- [3] S. Bjørnholm and J. E. Lynn, Rev. Mod. Phys. **52**, 725 (1980).
- [4] S. Åberg, Phys. Rev. Lett. **82**, 299 (1999).
- [5] R. G. Henry *et al.*, Phys. Rev. Lett. **73**, 777 (1994).
- [6] A. Lopez-Martens *et al.*, Phys. Rev. Lett. **77**, 1707 (1996).
- [7] A. Lopez-Martens *et al.*, Nucl. Phys. A **647**, 217 (1999).
- [8] T. Lauritsen *et al.*, Phys. Rev. C **62**, 044316 (2000).
- [9] I.-Y. Lee, Nucl. Phys. A **520**, 641c (1990).
- [10] D. G. Sarantites *et al.*, Nucl. Instrum. Methods Phys. Res., Sect. A **381**, 418 (1996).
- [11] C. Andreoiu *et al.*, Eur. Phys. J. A **14**, 317 (2002).
- [12] D. Bazzacco *et al.*, Phys. Rev. C **49**, R2281 (1994).
- [13] T. Bengtsson and I. Ragnarsson, Nucl. Phys. A **436**, 14 (1985).
- [14] A. V. Afanasjev *et al.*, Phys. Rep. **322**, 1 (1999).
- [15] D. Rudolph *et al.*, Phys. Rev. Lett. **89**, 022501 (2002).
- [16] W. D. Meyers and W. J. Swiatecki, Ark. Fys. **36**, 343 (1967).
- [17] I. Ragnarsson *et al.*, in *Proceedings of the International Conference on Frontiers of Nuclear Structure, Berkeley, California, 2002*, AIP Conf. Proc. No. 656, edited by P. Fallon and R. Clark (AIP, New York, 2002), p. 205.
- [18] B. Lauritsen *et al.*, Nucl. Phys. A **457**, 61 (1986).
- [19] S. Åberg, Phys. Rev. Lett. **64**, 3119 (1990).
- [20] M. Matsuo *et al.*, Nucl. Phys. A **617**, 1 (1997).